Aminoglycoside-mediated promotion of translation readthrough occurs through a non-stochastic mechanism that competes with translation termination

H.M. Chowdhury [1], M. A. Siddiqui [1], S. Kanneganti [1], N. Sharmin [2] , M. W. Chowdhury [2] and Md. Talat Nasim [1, 2, 3,4]*

[1] Department of Medical and Molecular Genetics, King's College London, London, United Kingdom, [2]School of Pharmacy and Medical Sciences, University of Bradford, Bradford, United Kingdom, [3]National Institute for Health Research (NIHR), Biomedical Research Centre, Guy's and St. Thomas' NHS Foundation Trust and King's College London, London, United Kingdom, [4]Centre for Health Agricultural and Socio-economic Advancements (CHASA), Lalmonirhat, Bangladesh.

Correspondence can be addressed to
*Dr. M. T. Nasim
School of Pharmacy and Medical Sciences
University of Bradford
Bradford BD7 1DP
United Kingdom
Tel. 01274 23 6076
Email. t.nasim@bradford.ac.uk

ABSTRACT

Attempts have been made to treat nonsense-associated genetic disorders by chemical agents and hence an improved mechanistic insight into the decoding of readthrough signals is essential for the identification and characterisation of factors for the treatment of these disorders. To identify either novel compounds or genes that modulate translation readthrough, we have employed dual reporter-based high-throughput screens that use enzymatic and fluorescence activities and screened bio-active NINDS compounds (n=1000) and siRNA (n=288) libraries. Whilst siRNAs targeting kinases such as CSNK1G3 and NME3 negatively regulate readthrough, neither the bio-active NINDS compounds nor PTC124 promote readthrough. Of note, PTC124 has previously been shown to promote readthrough. Furthermore, the impacts of G418 on the components of eukaryotic selenocysteine incorporation machinery have also been investigated. The selenocysteine machinery decodes the stop codon UGA specifying selenocysteine in natural selenoprotein genes. We have found that the eukaryotic *Sel*C gene promotes the selenocysteine insertion sequence (SECIS)-mediated readthrough but inhibits the readthrough activity induced by G418. We have previously reported that SECIS-mediated readthrough at UGA codons follows a non-processive mechanism. Here, we show that G418-mediated promotion of readthrough also occurs through a non-processive mechanism which competes with translation termination. Based on our observations, we suggest that proteins generated through a non-processive mechanism may be therapeutically beneficial for the resolution of nonsense-associated genetic disorders.

INTRODUCTION

There are more than 2500 genetic disorders caused by introduction of pre-mature termination codons (PTCs) into the reading frame. Examples of nonsense-associated genetic disorders include pulmonary arterial hypertension (PAH), cystic fibrosis, Duchene muscular dystrophy, Usher and Hurler syndromes. Human genes cannot normally be translated with in-frame stop codons with the exception of selenoprotein genes, which contain stop signals within their coding sequences. Decoding of the in-frame stop signal UGA occurs through a quaternary complex consisting of a specialised selenocysteine $tRNA^{Sec}$ (*Sel*C), specific elongation factors, a specific RNA secondary structure (SECIS), and GTP (1-3). This in association with ribosomes, decodes the UGA signal to selenocysteine (4,5). Both similarities and dissimilarities have been observed between SECIS- and aminoglycosides-mediated promotion of readthrough events. For example, the fourth bases located immediately after the in-frame termination codon affect the efficiency of readthrough. Pyrimidines (cytosine and uracil) as a fourth base promote both SECIS and aminoglycosides-mediated readthrough (1). Whilst aminoglycoside-mediated decoding of stop signals requires near cognate tRNA-codon interactions (6), selenocysteine incorporation requires the very specific $tRNA^{sec}$ (1-3). Although SECIS elements in the SELENOP*(SelP)* (7) gene can decode 10 in-frame stop codons to make selenoprotein P, it is not known whether the readthrough agents can decode multiple stop signals. Hence, an improved understanding of decoding of nonsense codons is essential for the identification and characterisation of small molecule agents for the treatment of PTC-associated genetic disorders.

Attempts have been made to identify small molecule compounds that promote translation readthrough of PTC-bearing transcripts aiming to resolve nonsense-associated disorders. To date, two high-throughput screens have been employed for the identification of small molecule agents that promote translation readthrough in mammalian cells (8,9). These screens are based on measuring the function of a single gene and hence are neither suitable for determining the efficiency of readthrough nor functional characterisation of readthrough-promoting chemicals. Firstly, they are prone to much intrinsic variability at

the levels of RNA stability and translation. Secondly, compounds such as PTC124 that modulate reporter activity may generate false positive results. While investigating the mode of action of PTC124, Auld et al. found that the compound is a potent luciferase inhibitor, which outcompetes with the assay reagent generating an increased luciferase read-out (8). To overcome these difficulties, PTT-ELISA has been developed (9). Major limitations of this technique are that (a) the method is single gene-based and (b) the activity is determined through a conjugation of multiple steps and hence is time consuming. We and others have developed dual readthrough reporters which by-pass the variables confounding the single reporter functions (1,10-13). No mammalian dual reporter-based high-throughput screening of trans-acting factors either for small molecule compounds or for short interfering RNAs (siRNAs) has been reported yet. Recently, a dual-fluorescence high-throughput screen has been reported but this system is limited to yeast cells (14). Hence, there is a need to develop dual reporter-based high-throughput screens in mammalian cells capable of bypassing the variables confounding single reporter functions.

In this report, we have developed mammalian cell-based dual-reporter screens and screened chemical (n=1000) and siRNA (n=288) libraries. We have found that siRNAs targeting the casein kinase 1 gamma 3 (CSNK1G3) and nucleotide diphosphate kinase 3 (NME3) genes may negatively regulate readthrough. Additionally, neither PTC124 nor the bio-active compounds collected by National Institute of Neurological Disease Syndrome (NINDS) promote translation readthrough. We have demonstrated that aminoglycosides promote both basal and SECIS-mediated translation readthrough. In contrast, the *Sel*C gene inhibited G418-mediated readthrough whilst the *Sel*D (Sephs2) gene elicited no discernible effects. Furthermore, we have found that G418 sulfate-mediated promotion of readthrough occurs through a non-stochastic mechanism and both translation termination and readthrough events compete with each other. Taken together, we propose a non-processive mechanism of translation readthrough as a therapeutic strategy for nonsense-associated genetic disorders.

RESULTS

Development of an enzyme-based dual reporter high-throughput screen for determining the efficiency of stop codon readthrough in mammalian cells

To overcome the limitations associated with single reporter-based high-throughput screens (8,9), we took advantage of our previously established dual-reporter assay based on genes encoding luciferase and β-galactosidase (1) . This reporter contains a segment harbouring an in-frame stop signal found within the selenoprotein phospholipid hydroperoxide glutathione peroxidase (*PHGPx*) gene. In the event of translation termination, β-gal protein is generated, whilst readthrough produces a β-gal and luciferase fusion protein (Figure 1A). The ratio of the activities of these two proteins thus determines the efficiency of readthrough. We first validated the assay system using G418 sulfate, an established agent known to promote translation readthrough. To rule out any construct specific effect, we used two reporter constructs with varying lengths of the *PHGP*x fragment. We found that G418 sulfate promoted readthrough of both constructs (Figure 1B). Next, the efficiency of readthrough was determined using a series of constructs harbouring an in-frame stop codon and compared efficiencies with a construct where the stop codon was changed to a cysteine codon (Figure 1C). We found the readthrough efficiency of a nonsense codon is in between 0.2-1% compared with a sense codon (Figure 1D and Supplementary Figures 1A-B). The validity of the sense codon containing protein was carried out by western blot analyses using anti-luciferase antibody which detected the 178 KDa luc-gal fusion protein (Supp Figure 1C).

We next investigated the effects of the so-called ‘fourth base’ located immediately after the UGA stop signal on readthrough efficiency. Constructs were generated with various fourth bases (Figure 1C) and their efficiencies were determined. Consistent with previous observations (15,16), we found that cytosine at the fourth base position promotes readthrough (Figure 1D and Supp Figure 1D) and G418-mediated readthrough is higher when pyrimidine instead of purine is the fourth base (Figure 1E). Western blot analyses

revealed higher level of luc-gal fusion protein in both UGAC and UGAU constructs following G418 treatment (Figure 1F).

For further validation, UGAG (Supp Figure 2A), UGAU (Supp Figure 2B) and UGAC (Supp Figure 2C) constructs were taken forward and cells overexpressing these constructs were treated with varying concentrations of G418 to determine their concentration dependent effects. G418 treatment promotes readthrough activities of all constructs in a concentration-dependent manner. Next, the effect of G418 was tested in a construct where the stop codon (UGAG) was changed to a cysteine codon (UGCG) (Supp Figure 2D). G418 treatment elicited no discernible effect on the UGCG construct. These data suggest the validity of readthrough and control constructs.

Having validated the readthrough assay, we investigated the effect of other aminoglycosides including gentamicin and tobramycin on readthrough efficiency. Cells treated with these aminoglycosides promoted readthrough efficiency of constructs where the fourth base was either purine (Supp Figure 2E) or pyrimidine (Supp Figure 2F). However, we noticed that tobramycin-mediated promotion of readthrough was at a lower level compared with that induced by either gentamicin or G418 sulfate.

The luc-gal based assay was further employed to investigate a number of nonsense alleles associated with cystic fibrosis, Duchene muscular dystrophy, Usher and Hurler syndrome. The nonsense codons (UGA or UAG) of the cystic fibrosis transmembrane conductance regulator (*CFTR*; p.G542X), alpha-L iduronidase (*IDUA*; p.Q70X), procadherin 15 (*PCDH*15; p.R245X) and dystrophin (*DMD*; p.R3381X) genes were introduced into the reading frames of lacZ and luciferase genes (Supp Figure 3A). HEK293T cells transiently transfected with these reporter constructs and treated with G418 sulfate showed an increase in the luc-gal ratio (Supp Figure 3B-F). Taken together, these data indicate the validity and usefulness of the luc-gal-based reporter assay for investigating the underlying mechanisms of readthrough for high-throughput screening of trans-acting factors.

Determination of readthrough activities of FDA-approved 1000 drugs

To re-purpose FDA approved drugs for the resolution of nonsense-associated disorders, we screened 1000 bioactive NINDS compounds (Supp Table 1) at 10 μM using the UGAU construct (Supp Figure 4). The rationale for selecting this construct is that the readthrough efficiency is higher when pyrimidine as the fourth base. We first determined the Z-factor value of this assay. The Z-factor value indicates the suitability of the assay for high-throughput screening (17). The Z-factor value of this assay was 0.51, which indicates that this is a good high-throughput assay. 39 compounds showing two-fold higher activity over the basal readthrough were taken forward and their efficiencies were determined in a 3-point concentration response curve (Supp Table 2). None of the hits promoted readthrough activity in a concentration-dependent manner, with the exception of peruvoside, which promoted the luc-gal ratio at the concentration of 10μM. Readthrough promoting activity of this compound was further validated using a different fourth base construct (UGAG) and a control construct with a sense codon (UGCG). The compound failed to promote readthrough activity of the UGAG construct while it inhibited luciferase and β-gal activities of the control UGCG construct (Supp Figure 5A). Further inspection revealed that the compound inhibited the β-galactosidase activities of UGAG, UGAC and the control UGCG constructs and luciferase activity of the control UGCG construct. Thus anti-luc-gal activities of the compound might have contributed to the increased luc-gal ratio (Supp Figure 5B-E). Additionally, whilst we found that 19 compounds inhibited readthrough activity at 0.1μM, ofloxacin and foscarnet sodium significantly inhibited readthrough at all concentrations used (0.1, 1 and 10μM) (Supp Table 2). Taken together, these data suggest that whilst the FDA approved NINDS drugs do not promote translation readthrough, some compounds within this collection may interfere with translation termination.

Identification of kinases that promote translation readthrough

We next wished to identify novel kinases capable of modulating translation readthrough by screening a siRNA library (On Target Plus, Dharmacon) which targets 288 kinases. The kinases were randomly selected and the library was screened in 384-well format in triplicate using the UGAU construct at a standard concentration of 30nM (Supp Figure

6A). The wells deviating three standard deviations were considered as hits (n=10) which were further validated using the siGENOME SMARTpool siRNAs (Dharmacon). The siGENOME SMARTpool is a mixture of 4 siRNAs, all designed to target different regions of the single gene of interest. siRNAs targeting the casein kinase 1 gamma 3 (CSNK1G3) and nucleotide diphosphate kinase 3 (NME3) genes significantly inhibited readthrough activity. In contrast, siRNAs targeting the other 8 genes and non-targeting control (NTC) siRNAs showed no discernible effects (Supp Figure 6B).

Development and validation of a dual-fluorescence readthrough reporter assay

Having established the enzyme-based screen, we next developed a dual-fluorescence-based readthrough assay aiming to investigate readthrough activity in single cells. The dual-fluorescence readthrough reporter is based on genes encoding DsRed-Express and EGFP. This assay was based on the same principle as used in the enzyme-based reporter with the exception that it harbours the *BMPR2* gene bearing a pathogenic nonsense mutation identified in a subject with pulmonary arterial hypertension (PAH). The reporter was developed such that, in the event of readthrough, a dual-fluorescent protein consisting of DsRed Express and EGFP is produced, whilst translation termination generates only the DsRed-Express protein. Thus, the ratio of the fluorescence intensities of these two proteins determines the efficiency of readthrough (Figure 2A).

The pTN139-PTC construct harbouring a nonsense codon expressed only the DsRed-Express protein, which following the treatment of G418 sulfate, generated both EGFP and DsRed-Express proteins (Figure 2B). Of note, we earlier confirmed by means of fluorescence microscopy (18), RT-PCR and western blot analyses that this nonsense mutation introduces a PTC (Supp Fig 7A-B). To determine the efficiency of readthrough at the level of single cells, HEK293T cells expressing fluorescence reporters were sorted using a fluorescence-activated cell sorter (FACS). Mock transfected cells produced little or no background fluorescence (Figure 2Ci) whilst cells containing the pTN139 construct generated the highest level of dual-fluorescence (Figure 2Civ). In contrast, cells bearing the 139-PTC construct generated little dual-fluorescence (Figure 2Cv). A significantly high proportion of the cells generated dual-fluorescence following gentamicin treatment

which validates the assay system (Figure 2Cvi and 2D). By determining the fluorescence intensity ratios of DsRed-Express to EGFP using a fluorescence plate reader, which indicates the degree of readthrough, we further confirmed that the assay detects gentamicin-mediated translation readthrough (Figure 2E).

We provided extensive evidence that there is a good correlation between the enzyme and fluorescence assays that fluorescence assay could be used as a secondary screen to verify the hits to reduce false positive and false negative results. Firstly, as the enzyme-based assay was based on the stop codon UGA, we mutated the UAG codon of the fluorescence reporter to UAA and UGA stop codons and determined their readthrough efficiencies in HEK293T cells. Consistent with existing literature, we found that the readthrough efficiency was higher when the internal stop signal was the UGA codon compared with that of either UAG or UAA codons (Supp Figure 7C) (19). Secondly, we tested a number of compounds including G418, gentamicin and peruvoside using the construct harbouring the UGA stop codon. Consistent with the luminescence data, the fluorescence results showed that aminoglycosides including G418 sulfate and gentamicin promoted readthrough, whilst peruvoside elicited no discernible effect (Supp Figure 8A).

PTC124 does not promote translation readthrough

We next determined the impact of PTC124 on readthrough and provided extensive evidence that this compound does not promote readthrough. First, the readthrough potential of PTC124 was investigated using the luc-gal-based double reporter readthrough assays. Briefly, constructs containing the nonsense codons (UGA or UAG) of the *CFTR*(p.G542X), *IDUA*(p.Q70X), *PCDH*15(p.R245X), *DMD*(p.R3381X) and *PHGPx*(p.59X) genes (Supp Figure 3A) were transiently transfected into HEK293T cells and treated with either G418 sulfate or PTC124. Cells treated with G418 sulfate showed an increase in the luc-gal ratio. In contrast, cells treated with PTC124 at 0.1, 1.0 and 10 μM, which elicit the most readthrough activity (20), failed to increase the luc-gal ratio (Figure 3A). Second, the influence of the fourth base on PTC124-mediated readthrough was investigated using the readthrough constructs where the fourth base immediately after the internal stop signal of the *PHGPx* gene was changed to adenosine (A), cytosine

(C) or uracil (U) (Figure 1C). A pyrimidine base as the fourth base resulted in a higher G418-mediated readthrough than a purine (Figure 1E), whilst PTC124 failed to promote luc-gal ratio of these constructs (Figure 3B). However, we noticed that PTC124 showed a tendency to reduce luc-gal ratio and in fact, this inhibition was significant at 10μM for UGAC. Next, the identity of the readthrough protein was verified by western blot analysis. As expected, G418 increased the production of the readthrough protein in the CFTR nonsense (p.G542X) construct while PTC124 generated no detectable full-length protein (Figure 3C). Finally, we tested PTC124 using fluorescence constructs harbouring either UAG or UGA or UAA stop codons and found that the agent at 10μM failed to promote readthrough of any of these fluorescence constructs (Supp Figure 8B).

Translation readthrough events compete with translation termination

The effect of release factors including *eRF*1 and 3 was investigated using a pyrimidine as the fourth base construct (UGAU). Overexpression of either *eRF*1 or *eRF*3 significantly reduces readthrough activity (Figure 4A). We found that knocking down of eRF1 using siRNA increased the readthrough activity (Figure 4B) which is inversely correlated with the overexpression experiment. However, siRNAs targeting eRF3 failed to elicit any discernible effects. Next, we investigated if the components of the eukaryotic selenocysteine incorporation machinery including the SECIS element, the $tRNA^{sec}$ (*Sel*C) and *Sel*D (Sephs2) promote readthrough activity. Consistent with previous observations, we found that incorporation of SECIS element at 3'UTR (Figure 4C) increased the activity of this UGA-SECIS construct up to 20 folds (Figure 4D), which was further increased when the cells were either treated with sodium selenite, an agent known to charge the $tRNA^{sec}$ in the absence and presence of *Sel*C (Figure 4E) or G418 sulfate (Figure 4F) (21-23). In contrast, overexpression of *Sel*C inhibited G418-induced readthrough activities whilst *Sel*D elicited no discernible effects (Figure 4G).

G418-promoted readthrough is significantly reduced at multiple stop signals

To develop an assay that can detect readthrough at multiple stop signals, we introduced three in-frame stop signals, one from the *PHGPx* and two from the selenoprotein P gene, into the enzyme-based reporter. Site-directed mutagenesis was carried out to create a

number of additional constructs that harbour various combinations of multiple in-frame stop signals (Figure 5A). The readthrough efficiency of these constructs was then determined in the absence and presence of G418 sulfate (400µg/ml). Both basal (Figure 5B) and G418-mediated readthrough (Figure 5C) were higher for transcripts containing one stop signal than for those containing two or more stop signals. Western blot analysis showed the production of the full-length fusion protein following G418 treatment when constructs containing one stop signal were used. In contrast, full length protein production was markedly reduced when constructs with two or three stop signals were employed (Figure 5D).

G418 sulfate inhibits excessive proliferation in primary mouse PASMCs

Finally, we investigated whether readthrough compounds elicit beneficial effects in a disease-relevant *ex vivo* cell-based assay. Primary PASMCs derived from mutant mice harbouring a pathogenic nonsense mutation (p.R899X) showed excessive proliferation compared with cells derived from wild-type animals and TGFβ1 stimulation further increased proliferation of mutant cells (Figure 6A, 6C), which are consistent to our previous observations (24,25). Treatment of cells with G418 inhibited excessive mutant cell proliferation (Figure 6A), whilst PTC124 failed to show any discernible effects on both wild-type and mutant cells (Figure 6B-C). However, the compound only at 10µM slightly inhibited excessive mutant cell proliferation induced by TGFβ1 stimulation (Figure 6C).

DISCUSSION

We present mammalian cell-based double reporter readthrough screens and provide novel mechanistic insights into the translation readthrough process. Whilst this study identifies kinases such as CS3K1G and NME3 as potential regulators, the bio-active NINDS compounds and PTC124 do not promote readthrough. Compounds within the NINDS collection including ofloxacin and foscarnet sodium may modulate the translation termination process. The *Sel*C gene, which encodes for the tRNA ^{sec} has opposing effects on readthrough. This tRNA promotes SECIS-mediated readthrough and inhibits the readthrough activity promoted by G418 sulfate. We have previously reported that SECIS-

mediated readthrough occurs through a non-processive mechanism (1). Here, we show that G418-mediated readthrough does not follow a stochastic process, rather it also follows a non-processive mechanism.

The limitations of currently used single reporter-based high-throughput screens (8,9) and the use of bi-cistronic reporters for investigating underlying mechanisms readthrough (1,10-13) prompted us to develop dual-reporter based screens. We have demonstrated a number of ways that our high-throughput screening assays bypass the limitations associated with single reporter functions. Firstly, our mammalian cell-based double-reporter screens minimize the variables such as variation between samples at the levels of transcription, RNA stability and translation. Secondly, since our techniques are based on measuring the ratio of two reporter activities, they are suitable for determining the efficiency of cis or trans-acting factors that affect either the translation termination or readthrough process. For example, compounds including ofloxacin and foscarnet sodium significantly reduced the readthrough efficiency which suggests that these molecules are likely to affect the translation termination process. Thirdly, false positive compounds that interact either with assay substrates or affect the activity of a reporter can easily be identified. We have provided extensive evidence that PTC124 does not promote readthrough and peruvoside is a potent β-galactosidase and luciferase inhibitor. Finally, whilst the enzyme-based assay provides higher sensitivity, the advantages of fluorescence-based assay are that the activity is measured in single cells without cell lysis and substrate addition (14) and the fluorescence assay can provide an additional mean to verify the hits to reduce false positive and false negative results.

However, these screens have several limitations. For example, the fluorescence-based assay was found to be less sensitive than the enzyme-based assay. The fluorescence-based assay is subject to interference from autofluorescence, which may interfere with eGFP fluorescence. This could be easily corrected by swapping eGFP for the DsRed-Express reporter. The drawbacks associated with the enzyme-based assay are that factors affecting luciferase or β-galactosidase activities may generate false positive or false negative results. These false positive or negative results could easily be detected using

control constructs harbouring a sense codon instead of a stop signal (Supp Figure 5A, D-E). However, these limitations are unlikely to affect the usefulness of these techniques as long as an independent method such as western blot analysis or RT-PCR is used to validate the positive hits identified through the initial screen. As our pilot screen detected established readthrough compounds, high-throughput screenings that employ a diverse set and a larger number of molecules are likely to identify novel readthrough agents.

The strategy of screening a pilot library collection identified NME3 and CSNK1G3 kinases as potential modulators of readthrough, suggesting that additional genes in this pathway would be likely to be identified from a genome-wide siRNA screen. NME3 plays a major role in the synthesis of nucleoside triphosphate and CSNK1G3 phosphorylates a large number of proteins such as caseins. However, further studies are required to establish their roles in readthrough and whether they present druggable targets for the resolution of nonsense-associated genetic disorders. Re-purposing of NINDS drugs for PTC-associated disorders is a distant possibility as these drugs do not harbour any readthrough promoting activity. PTC124 has been shown to elicit beneficial effects in cystic fibrosis and Duchene muscular dystrophy model systems (26,27) but its inability to promote readthrough in cell-based assays and failure to restore cellular defects in the mouse PASMCs harbouring a nonsense mutation support the finding that this agent is not a general promoter of readthrough. Non-antibiotic compounds have been identified all the time and some of these chemicals have been tested in preclinical and clinical trials (9,28). Failure of PTC124 in this and other assays (8,29) emphasize the need for further investigation of these readthrough agents including their mode of action and impact on processivity prior to testing them in animals and in clinical trials.

It is essential to determine whether the readthrough-promoting chemicals follow a processive or non-stochastic mechanism as each of these mechanisms is likely to impact on the therapeutic efficacy of the readthrough agents. In the processive model, the agent decodes the PTC by re-programming the translating ribosomes. When a second stop signal enters the ribosomal A site, the re-programming ribosomes decode the stop signal with the same efficiency as the first stop codon (Figure 7A-B). Processivity is the likely

explanation for decoding of 10 in-frame stop signals found in the SELENOP gene (1). In contrast, in the non-stochastic model, the readthrough agent transiently associates with the translating ribosomes, decodes the stop signal with a sub-optimal efficiency and dissociates from the complex once decoding is completed (Figure 7C-D). When a second stop signal enters the ribosomal A sites, the decoding complex needs to be formed again. Efficiency of decoding of both stop signals will be the cumulative product of all incorporation efficiencies. G418-mediated promotion of readthrough is significantly reduced in the presence of two or three stop signals, which suggests that aminoglycoside-mediated readthrough does not follow the processive mechanism rather the readthrough occurs through a non-stochastic process. We have previously reported that SECIS-mediated readthrough also follows a non-processive mechanism (1). Taken together, it appears that proteins generated through a non-processive mechanism, may be therapeutically beneficial compared with those generated via the processive model for a number of reasons. Firstly, the probability for the generation of an extended protein that bypasses the bonafide stop signal in a PTC harbouring transcript is relatively low as the readthrough efficiency is directly proportional to the multiplicative product of all readthrough efficiencies. Secondly, the extended protein is likely to be decayed due to the presence of unstable peptides derived from the translation of 3'UTR (30). Finally, the processive mechanism is likely to generate proteins, which will harbour more mutated amino acid residues compared with the proteins generated through the non-stochastic process.

Furthermore, we show that the efficiency of a stop codon readthrough is below 1% and that pyrimidine residues in the 'fourth base' position relative to the internal stop signal promote both basal and aminoglycoside-mediated readthrough, which all are in line with previous observations (15,31,32). G418-mediated readthrough efficiency is higher in the presence of a pyrimidine, which may favour the recruitment of suppressor tRNAs to the stop signal (33,34). In contrast, in the presence of a purine, which favours the binding of release factors to the stop signal (35), G418-promoted readthrough was significantly reduced. In the presence of release factors *eRF*1 and *eRF*3, both basal and G418-induced readthrough events are significantly reduced suggesting a direct competition between

termination and readthrough events (36,37). Aminoglycosides have been suggested to promote translation readthrough and selenocysteine incorporation (21-23) by interfering with translation elongation (38,39). The inability of $tRNA^{sec}$ to promote both basal and aminoglycoside mediated readthrough suggests its specificity for decoding stop signals.

In conclusion, we report a number of useful screens and assays for determining the efficiency and investigating the underlying mechanisms of translation readthrough in mammalian cells. We have demonstrated that neither PTC124 nor the bio-active NINDS drugs promote readthrough. Compounds within the NINDS collection including ofloxacin and foscarnet sodium and kinases such as NME3 and CSNK1G3 may regulate the translation termination machinery. Furthermore, we have found that aminoglycosides-mediated promotion of readthrough occurs through a non-processive mechanism that competes with translation termination. Molecules with improved suppression activity that follow the non-processive mechanism should expand the utility of inducers of readthrough to control translation-based gene regulation and may have important clinical applications for the treatment of PTC-associated genetic disorders.

MATERIALS AND METHODS

Compounds

G418 sulfate and gentamicin were purchased from Promega and PTC124 was purchased from Selleckchem. G418 and gentamicin were dissolved in water whilst PTC124 was in DMSO. All chemicals were kept at -20^{o}C until use.

Plasmid construction

Nucleotide sequences correspond to amino acids from 526 to 559 of human *CFTR* (MIM:602414), from 229 to 262 of *PCDH*15 (MIM:605514), from 3365 to 3398 of *DMD* (MIM:300377) and from 54 to 87 of *IDUA* (MIM:252800) genes harbouring the nonsense codons were cloned into *Sal*I and *BamH*I sites of pBPLUGA (10) and the respective clones were verified by sequencing (DNA cloning Service, Germany). The details of the other luc-gal-based reporter constructs were published earlier (1,10).

Single-cell based dual-fluorescence readthrough assay constructs were generated in several steps. First, the pEGFP gene was cloned into the BamHI and XbaI sites of the DsRed-Express-C1plasmid (Clonetech), which resulted in the DsRed Express-EGFP vector. Next, the exon 9 of plasmid pTN136 (18) was replaced with exon 12 of *BMPR2* gene using PCR mutagenesis (40). The resultant splicing unit was cloned into XhoI and BamHI sites of the DsRed Express-EGFP vector and designated as pTN139. Finally, plasmid pTN139PTC was generated by substituting 'T' with 'G' at position 2620 of the exon 12 such that, it introduced a stop signal (TAG) (18). Site directed mutagenesis was initiated to change the TAG codon to TAA and TGA codons.

Cell culture, transient transfection, treatment of cells with chemical agents, enzymatic and fluorescence assays and western blots

Cell culture and transfections were carried out as described elsewhere (41), (42-44). The amount of plasmid DNA transfected into the HEK293 and HEK293T cell lines varied from assay to assay (from 30 ng to 1 μg). 24 hours after transfection, cells were treated with compounds in DMEM containing 0.1% FBS for an additional 24 hours. Cell lysate was prepared as described earlier (24,25) and Luciferase and β-galactosidase activities were determined with the Dual-light Reporter Assay (Applied Biosystems) using an ORION-II Plate Luminometer (Berthold) according to the manufacturer's protocols. For determination of fluorescence intensity, cells were grown in 96 well black plates and 24 hours after transfection, cells were treated with compounds in DMEM containing 0.1% FBS, and grown for an additional 48 hours. At the time of measurement, the medium was discarded and the fluorescence intensities were determined using BMG Labtech Omega fluorescence plate reader. Fluorescence microscopy and fluorescence activated cell sorting (FACS) were carried out as described elsewhere (41-44). Western blots were carried out using anti-luciferase (Calbiochem) and anti-GFP (AbCam) antibodies following manufacturer's protocols. To confirm equal loading, the membranes were stripped and re-probed with anti-β-actin antibody (Cell Signaling).

RNA isolation, cDNA synthesis and reverse Transcriptase PCR (RT-PCR)

RNA was isolated from mammalian cells using either TRI-Reagent (Sigma) or RNeasy Purification kit (Qiagen). cDNA was synthesized using random primers and M-MLV Reverse Transcriptase (Promega) following the manufacturer's protocol. The PCR was carried out using Hi-Fidelity Extensor Master Mix (ABgene).

Screening of small molecule compounds

Screening of the NINDS was carried out in HEK293T cells in 96-well plate format. 10,000 cells were grown in half area 96 well clear plates and 24 hours after seeding cells in each well were transfected with 25ng of readthrough reporter plasmid using Gene Jammer Transfection Reagent (Stratagene) following manufacturer's protocol. 24 hours after transfection, cells were treated with compounds (10μM) in DMEM containing 0.1% FBS, and grown for an additional 24 hours. Cell lysate was prepared using Reporter Lysis Buffer (Promega) and the lysate was transferred to white plates and luc-gal activities were measured as described above.

siRNA screening and hit validation

The siRNA screen in mammalian cells was carried out at the Sheffield siRNA Screening Facility, University of Sheffield. The luc-gal-based readthrough assay system containing pyrimidine as the fourth base (UGAC construct) was employed. A total of 288 siRNAs were screened in 384-well format in triplicate in HEK293T cells. Briefly, HEK293T cells were transfected with UGAC plasmid in T75 flasks and 24 hours following transfection, the cells were reverse transfected with siRNAs in 384-well format using Dharmafect1 (Dharmacon). Three days following siRNA transfection (30nM), the cells were harvested and their luc-gal activities were determined using a Varioskan SK plate reader (Thermo). For the primary screen, On Target Plus siRNA library (Dharmacon) was used, containing a pool of four individual siRNAs per gene. The wells deviating 3 standard deviations (3SD) were considered as hits and the hits were validated using siGENOME SMART pool siRNAs (Dharmacon) at a concentration of 30nM in 96-well format. siGENOME SMART pool siRNAs (Dharmacon) at a concentration of 30nM were used to knock down eRF1 and eRF3 genes.

Quantitation of proliferation of mouse primary PASMCs

Quantitation of cell proliferation was carried out as described elsewhere (24,25). Briefly, mouse PASMCs were grown in 96-well plates. Cells were treated with either G418 sulfate or PTC124 in DMEM containing 0.1% FBS and grown for an additional three days. Relative rate of proliferation was carried out using CellTiter 96® Aq_{ueous} One Solution Cell Proliferation Assay (Promega) following manufacturer's instruction.

Statistics

Statistical analysis was performed following paired Student's t-test. The Z-factor was calculated following a protocol described elsewhere (17). Comparison of multiple means was carried out using ANOVA followed by Tukey's post hoc test.

FIGURE LEGENDS

Figure 1

(A) An outline of the enzyme activity reporter. In brief, translation termination in the internal stop signal generates the β-gal protein. In the event of readthrough, a β-gal-luciferase fusion protein will be produced. Thus, the ratio of the two reporter activities indicates the efficiency of readthrough. Two independent constructs, H8 (pBPLUGA; (10)) and H8A (1), were used in this study to rule out any construct specific effect. Construct H8 contains a 17 bp fragment of the *PHGPx* gene harbouring an in-frame stop signal whilst H8A contains a 91 bp DNA fragment. The luc-gal ratio was markedly increased in both constructs following G418 sulfate (400μg/ml) treatment (B). An outline of the constructs to determine the effect of 'fourth bases' on stop readthrough (C). The stop codon UGA was changed to a cysteine (UGU) codon and the fourth base 'G' was changed to either 'A' or 'C' or 'U' as indicated by arrows. The efficiency of stop codon readthrough (D) and the effect of the 'fourth base' on both basal and G418 sulfate-mediated (E) translation readthrough. Western blot analysis of proteins generated from pyrimidine harbouring constructs (UGAC and UGAU) in the absence and presence of G418 treatment (F).**P<0.01 and ***P<0.001 compared with untreated control.

Figure 2

Determination of readthrough in single cells. An outline of the fluorescence-based translation readthrough assay (A). The principle of the reporter system is similar to that mentioned in Figure 1 with the exception that it contains a translation termination signal in exon 12 of the *BMPR2* gene and that luciferase and β-galactosidase genes are replaced by genes encoding EGFP and DsRed-Express proteins. Exon 12 of *BMPR2* is fused in-frame to an adenovirus splicing unit (41) so that it generates a DsRed-EGFP fusion protein. Introduction of a premature termination codon (PTC) into exon 12 leads to the production of the DsRed-Express protein only. Live cell imaging of G418 sulfate untreated (upper panel) and treated (400μg/ml) (lower panel) HEK293T cells transfected with the PTC containing construct (139PTC) (B). Determination of readthrough by FACS analysis (C). Cells transfected with pTN139 generated the highest proportion of dual-fluorescence cells (Civ), whilst 139PTC produced few dual-fluorescence cells (Cv). The population of 139PTC-derived dual-fluorescence cells was markedly increased following gentamicin (Cvi and E) treatment (600μg/ml). EGFP- (Cii) and DsRed-Express– (Ciii) expressing cells were used as fluorescence positive controls, whilst mock transfected cells (Ci) were used as a negative control. Cells expressing the 139-PTC construct treated with gentamicin showed increased the ratio of eGFP-DsRed fluorescence intensities (D) and the number of dual-fluorescence cells (E) as determined by a fluorescence plate reader and FACS analysis, respectively. Values derived from untreated cells were set as 100. **P<0.01 compared with untreated control.

Figure 3

PTC124 fails to promote translation readthrough. HEK293T cells transiently transfected with human *CFTR* (p.G542X), *PCDH*15 (p.R245X), *DMD* (p.R3381X), *IDUA* (p.Q70X), or pig *PHGPx* (p.59X) were treated with G418 (400μg/ml) or increasing concentrations of PTC124 (A). Cells were transfected with various *PHGPx* constructs (p.59X) containing adenosine (A), cytosine (C), guanine (G) or thiamine (T) in the fourth base position (underlined) and were treated with G418 (400μg/ml) (B) or increasing concentrations of PTC124 (B). Western blot analysis of HEK293T cells transiently

transfected with the *CFTR* (p.G542X) dual reporters following treatment with G418 or increasing concentrations of PTC124 for luciferase and β-actin proteins (C). The dual reporter generated a fusion protein of approximately 178 KDa. G418 not PTC124 increased the expression of this protein in cells transfected with *CFTR* nonsense (p.G542X) construct. *** P< 0.001, NS- non-significant compared with untreated cells.

Figure 4

Competition between translation readthrough and termination events. Effects of *eRF*1 and 3 on readthough by means of plasmid overexpression (A) and siRNA knock down (B) determined by enzyme-based assay using the UGAU construct. An outline of SECIS-mediated readthrough construct where the SECIS element was introduced in the 3'UTR (C). Readthrough efficiency of the UGAG-SECIS construct compared with the construct without the SECIS element (D). Effects of *Sel*C and Na_2SO_3 (2μM) (E) and G418 (400μg/ml) (F) on SECIS-mediated readthrough. Effects of *Sel*C and *Sel*D on both basal and G418-mediated readthrough assessed on the UGAU construct (G). ** P< 0.01, ***p < 0.001 compared with untreated cells. NS- non-significant.

Figure 5

Translation readthrough at successive PTCs. (A) A segment of the *SELENOP* gene (accession number z11793; from nucleotides 934–990) containing two UGA codons was inserted into the enzyme-based reporter (Figure 1A). The diagram indicates the relative positions of the *PHGPx* and *SELENOP* UGA codons. PTC and sense codon are indicated by 'I' and 'O', respectively. Translation readthrough at multiple sites in the absence (B) and presence of G418 treatment (C). (D) Western blot analysis of readthrough protein detected by anti-luciferase antibody. G418-mediated readthrough resulted in the production of the gal-luc fusion protein in the presence of one PTC but not two or three PTCs (Upper panel). The blot was stripped and reprobed with β-actin antibody (lower panel) to demonstrate equal loading. The control cells were mock transfected. **P<0.01 and ***P<0.001 compared with IOO construct (B). ***P<0.001 compared with constructs containing one stop signal (C).

Figure 6

Resolution of nonsense-associated cellular defects using readthrough compounds. (A) Inhibition of excessive cell proliferation by aminoglycosides. The relative rate of proliferation in wild-type (WT *bmpr2* $^{+/+}$) and mutant (*bmpr2* $^{R899X+/-}$) mouse primary PASMCs. Effects of G418 sulfate on proliferation of both wild-type and mutant PASMCs. ***P<0.001 compared with untreated control. Effects of PTC124 on wild type (B) and mutant PASMCs following TGFβ1 stimulation (C). Concentrations of the compound and the ligand are indicated below graphs. *P<0.05 compared with cells stimulated with TGFβ1.

Figure 7

Processive and non-processive models of translation readthrough. A diagram depicting normal translation termination showing dissociation of translating ribosomes (A). Processive model of readthrough in transcripts harbouring a PTC (B). Translating ribosomes associate with transcripts whereby the 3'UTR together with readthrough complex determines the efficiency of decoding of all successive in-frame stop signals. Processivity is the likely explanation for the synthesis of selenoprotein P, which contains 10 in-frame stop signals. Non-processive mechanism of readthough in transcripts with a PTC where ribosomes dissociate both at PTC and stop signals in the absence (C) and presence (D) of a readthrough agent. In non-processive model, production of readthrough proteins are directly proportional to multiplicative sum of all incorporation efficiencies and polypeptides that bypass stop signal are likely to be degraded due to the presence of destabilizing peptides at the C-terminal end (30). Downward and rightwards arrows indicate the efficiency of translation termination and readthrough, respectively. RA-readthrough agents, UTR- untranslated region,

FUNDING

This work was supported by a fellowship (awarded to MTN) from the Department of Health via the NIHR Comprehensive Biomedical Research Centre award to Guy's & St Thomas' NHS Foundation Trust in partnership with King's College London, Heptagon Life Science Proof of Concept Fund (grant KCL24 to MTN), the Great Britain Sasakawa

Foundation (grant B70 to MTN), the Royal Society (grant 43049 to MTN) and the University of Bradford (grants 003200 and DH005 to MTN).

ACKNOWLEDGEMENTS

The mouse PASMCs were generous gifts from Prof. N.W. Morrell (Cambridge). The authors wish to thank Dr. P. Di Meglio (King's College London), A. Siskoglou (Leicester) for valuable technical assistance, Miss L. N'Koy and Dr. Stephen Brown at the Sheffield RNAi Screening Facility for library design.

COMPETING INTERESTS STATEMENT: None

REFERENCES

1. Nasim, M.T., Jaenecke, S., Belduz, A., Kollmus, H., Flohe, L. and McCarthy, J.E. (2000) Eukaryotic selenocysteine incorporation follows a nonprocessive mechanism that competes with translational termination. *J Biol Chem*, **275**, 14846-14852.
2. Berry, M.J. (2005) Knowing when not to stop. *Nat Struct Mol Biol*, **12**, 389-390.
3. Low, S.C. and Berry, M.J. (1996) Knowing when not to stop: selenocysteine incorporation in eukaryotes. *Trends Biochem Sci*, **21**, 203-208.
4. Bock, A., Forchhammer, K., Heider, J., Leinfelder, W., Sawers, G., Veprek, B. and Zinoni, F. (1991) Selenocysteine: the 21st amino acid. *Mol Microbiol*, **5**, 515-520.
5. Rother, M., Resch, A., Wilting, R. and Bock, A. (2001) Selenoprotein synthesis in archaea. *Biofactors*, **14**, 75-83.
6. Roy, B., Leszyk, J.D., Mangus, D.A. and Jacobson, A. (2015) Nonsense suppression by near-cognate tRNAs employs alternative base pairing at codon positions 1 and 3. *Proc Natl Acad Sci U S A*, **112**, 3038-3043.
7. Gladyshev, V.N., Arner, E.S., Berry, M.J., Brigelius-Flohe, R., Bruford, E.A., Burk, R.F., Carlson, B.A., Castellano, S., Chavatte, L., Conrad, M. *et al.* (2016) Selenoprotein Gene Nomenclature. *J Biol Chem*, **291**, 24036-24040.
8. Auld, D.S., Thorne, N., Maguire, W.F. and Inglese, J. (2009) Mechanism of PTC124 activity in cell-based luciferase assays of nonsense codon suppression. *Proc Natl Acad Sci U S A*, **106**, 3585-3590.
9. Du, L., Damoiseaux, R., Nahas, S., Gao, K., Hu, H., Pollard, J.M., Goldstine, J., Jung, M.E., Henning, S.M., Bertoni, C. *et al.* (2009) Nonaminoglycoside compounds induce readthrough of nonsense mutations. *J Exp Med*, **206**, 2285-2297.

10. Kollmus, H., Flohe, L. and McCarthy, J.E. (1996) Analysis of eukaryotic mRNA structures directing cotranslational incorporation of selenocysteine. *Nucleic Acids Res*, **24**, 1195-1201.
11. Grentzmann, G., Ingram, J.A., Kelly, P.J., Gesteland, R.F. and Atkins, J.F. (1998) A dual-luciferase reporter system for studying recoding signals. *Rna*, **4**, 479-486.
12. Harger, J.W. and Dinman, J.D. (2004) Evidence against a direct role for the Upf proteins in frameshifting or nonsense codon readthrough. *Rna*, **10**, 1721-1729.
13. Cardno, T.S., Poole, E.S., Mathew, S.F., Graves, R. and Tate, W.P. (2009) A homogeneous cell-based bicistronic fluorescence assay for high-throughput identification of drugs that perturb viral gene recoding and read-through of nonsense stop codons. *Rna*, **15**, 1614-1621.
14. Altamura, E., Borgatti, M., Finotti, A., Gasparello, J., Gambari, R., Spinelli, M., Castaldo, R. and Altamura, N. (2016) Chemical-Induced Read-Through at Premature Termination Codons Determined by a Rapid Dual-Fluorescence System Based on S. cerevisiae. *PLoS One*, **11**, e0154260.
15. McCaughan, K.K., Brown, C.M., Dalphin, M.E., Berry, M.J. and Tate, W.P. (1995) Translational termination efficiency in mammals is influenced by the base following the stop codon. *Proc Natl Acad Sci U S A*, **92**, 5431-5435.
16. Howard, M.T., Shirts, B.H., Petros, L.M., Flanigan, K.M., Gesteland, R.F. and Atkins, J.F. (2000) Sequence specificity of aminoglycoside-induced stop condon readthrough: potential implications for treatment of Duchenne muscular dystrophy. *Ann Neurol*, **48**, 164-169.
17. Zhang, J.H., Chung, T.D. and Oldenburg, K.R. (1999) A Simple Statistical Parameter for Use in Evaluation and Validation of High Throughput Screening Assays. *J Biomol Screen*, **4**, 67-73.
18. Nasim, M.T., Ghouri, A., Patel, B., James, V., Rudarakanchana, N., Morrell, N.W. and Trembath, R.C. (2008) Stoichiometric imbalance in the receptor complex contributes to dysfunctional BMPR-II mediated signalling in pulmonary arterial hypertension. *Hum Mol Genet*, **17**, 1683-1694.
19. Loughran, G., Chou, M.Y., Ivanov, I.P., Jungreis, I., Kellis, M., Kiran, A.M., Baranov, P.V. and Atkins, J.F. (2014) Evidence of efficient stop codon readthrough in four mammalian genes. *Nucleic Acids Res*, **42**, 8928-8938.
20. Welch, E.M., Barton, E.R., Zhuo, J., Tomizawa, Y., Friesen, W.J., Trifillis, P., Paushkin, S., Patel, M., Trotta, C.R., Hwang, S. *et al.* (2007) PTC124 targets genetic disorders caused by nonsense mutations. *Nature*, **447**, 87-91.
21. Handy, D.E., Hang, G., Scolaro, J., Metes, N., Razaq, N., Yang, Y. and Loscalzo, J. (2006) Aminoglycosides decrease glutathione peroxidase-1 activity by interfering with selenocysteine incorporation. *J Biol Chem*, **281**, 3382-3388.
22. Tobe, R., Naranjo-Suarez, S., Everley, R.A., Carlson, B.A., Turanov, A.A., Tsuji, P.A., Yoo, M.H., Gygi, S.P., Gladyshev, V.N. and Hatfield, D.L. (2013) High error rates in selenocysteine insertion in mammalian cells treated with the antibiotic doxycycline, chloramphenicol, or geneticin. *J Biol Chem*, **288**, 14709-14715.
23. Martitz, J., Hofmann, P.J., Johannes, J., Kohrle, J., Schomburg, L. and Renko, K. (2016) Factors impacting the aminoglycoside-induced UGA stop codon

readthrough in selenoprotein translation. *Journal of trace elements in medicine and biology : organ of the Society for Minerals and Trace Elements*, **37**, 104-110.
24. Nasim, M.T., Ogo, T., Chowdhury, H.M., Zhao, L., Chen, C.N., Rhodes, C. and Trembath, R.C. (2012) BMPR-II deficiency elicits pro-proliferative and anti-apoptotic responses through the activation of TGFbeta-TAK1-MAPK pathways in PAH. *Hum Mol Genet*, **21**, 2548-2558.
25. Ogo, T., Chowdhury, H.M., Yang, J., Long, L., Li, X., Torres Cleuren, Y.N., Morrell, N.W., Schermuly, R.T., Trembath, R.C. and Nasim, M.T. (2013) Inhibition of Overactive Transforming Growth Factor-beta Signaling by Prostacyclin Analogs in Pulmonary Arterial Hypertension. *Am J Respir Cell Mol Biol*, **48**, 733-741.
26. Du, M., Liu, X., Welch, E.M., Hirawat, S., Peltz, S.W. and Bedwell, D.M. (2008) PTC124 is an orally bioavailable compound that promotes suppression of the human CFTR-G542X nonsense allele in a CF mouse model. *Proc Natl Acad Sci U S A*, **105**, 2064-2069.
27. Kayali, R., Ku, J.M., Khitrov, G., Jung, M.E., Prikhodko, O. and Bertoni, C. (2012) Read-through compound 13 restores dystrophin expression and improves muscle function in the mdx mouse model for Duchenne muscular dystrophy. *Hum Mol Genet*, **21**, 4007-4020.
28. Keeling, K.M. and Bedwell, D.M. (2011) Suppression of nonsense mutations as a therapeutic approach to treat genetic diseases. *Wiley Interdiscip Rev RNA*, **2**, 837-852.
29. McElroy, S.P., Nomura, T., Torrie, L.S., Warbrick, E., Gartner, U., Wood, G. and McLean, W.H. (2013) A lack of premature termination codon read-through efficacy of PTC124 (Ataluren) in a diverse array of reporter assays. *PLoS Biol*, **11**, e1001593.
30. Arribere, J.A., Cenik, E.S., Jain, N., Hess, G.T., Lee, C.H., Bassik, M.C. and Fire, A.Z. (2016) Translation readthrough mitigation. *Nature*, **534**, 719-723.
31. Bidou, L., Hatin, I., Perez, N., Allamand, V., Panthier, J.J. and Rousset, J.P. (2004) Premature stop codons involved in muscular dystrophies show a broad spectrum of readthrough efficiencies in response to gentamicin treatment. *Gene Ther*, **11**, 619-627.
32. Manuvakhova, M., Keeling, K. and Bedwell, D.M. (2000) Aminoglycoside antibiotics mediate context-dependent suppression of termination codons in a mammalian translation system. *RNA*, **6**, 1044-1055.
33. Bonetti, B., Fu, L., Moon, J. and Bedwell, D.M. (1995) The efficiency of translation termination is determined by a synergistic interplay between upstream and downstream sequences in Saccharomyces cerevisiae. *J Mol Biol*, **251**, 334-345.
34. Poole, E.S., Brown, C.M. and Tate, W.P. (1995) The identity of the base following the stop codon determines the efficiency of in vivo translational termination in Escherichia coli. *Embo J*, **14**, 151-158.
35. Bulygin, K.N., Khairulina, Y.S., Kolosov, P.M., Ven'yaminova, A.G., Graifer, D.M., Vorobjev, Y.N., Frolova, L.Y., Kisselev, L.L. and Karpova, G.G. Three distinct peptides from the N domain of translation termination factor eRF1 surround stop codon in the ribosome. *Rna*, **16**, 1902-1914.

36. Drugeon, G., Jean-Jean, O., Frolova, L., Le Goff, X., Philippe, M., Kisselev, L. and Haenni, A.L. (1997) Eukaryotic release factor 1 (eRF1) abolishes readthrough and competes with suppressor tRNAs at all three termination codons in messenger RNA. *Nucleic Acids Res*, **25**, 2254-2258.
37. Janzen, D.M. and Geballe, A.P. (2004) The effect of eukaryotic release factor depletion on translation termination in human cell lines. *Nucleic Acids Res*, **32**, 4491-4502.
38. Eustice, D.C. and Wilhelm, J.M. (1984) Fidelity of the eukaryotic codon-anticodon interaction: interference by aminoglycoside antibiotics. *Biochemistry*, **23**, 1462-1467.
39. Bar-Nun, S., Shneyour, Y. and Beckmann, J.S. (1983) G-418, an elongation inhibitor of 80 S ribosomes. *Biochim Biophys Acta*, **741**, 123-127.
40. Nasim, M.T., Eperon, I.C., Wilkins, B.M. and Brammar, W.J. (2004) The activity of a single-stranded promoter of plasmid ColIb-P9 depends on its secondary structure. *Mol Microbiol*, **53**, 405-417.
41. Nasim, M.T., Chowdhury, H.M. and Eperon, I.C. (2002) A double reporter assay for detecting changes in the ratio of spliced and unspliced mRNA in mammalian cells. *Nucleic Acids Res*, **30**, e109.
42. Nasim, M.T., Chernova, T.K., Chowdhury, H.M., Yue, B.G. and Eperon, I.C. (2003) HnRNP G and Tra2beta: opposite effects on splicing matched by antagonism in RNA binding. *Hum Mol Genet*, **12**, 1337-1348.
43. Nasim, M.T. and Trembath, R.C. (2005) A dual-light reporter system to determine the efficiency of protein-protein interactions in mammalian cells. *Nucleic Acids Res*, **33**, e66.
44. Paillusson, A., Hirschi, N., Vallan, C., Azzalin, C.M. and Muhlemann, O. (2005) A GFP-based reporter system to monitor nonsense-mediated mRNA decay. *Nucleic Acids Res*, **33**, e54.

Figure 1

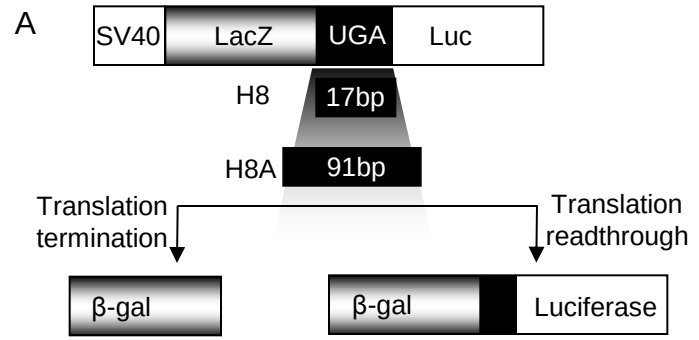
A
SV40
LacZ
UGA
Luc
H8
17bp
H8A
91bp
Translation termination
Translation readthrough
β-gal
β-gal
Luciferase

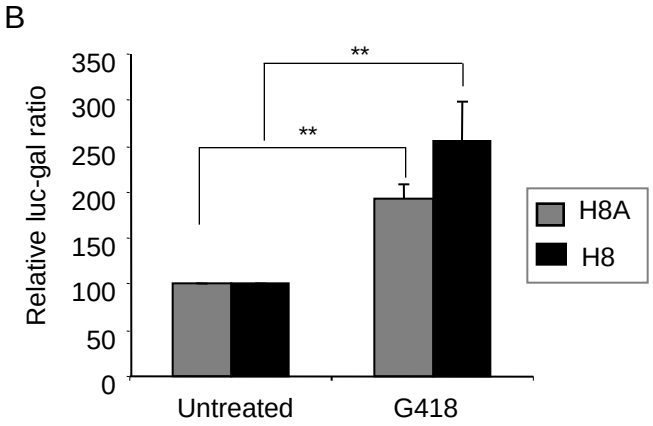
B
Relative luc-gal ratio
350
300
250
200
150
100
50
0
**
**
H8A
H8
Untreated
G418

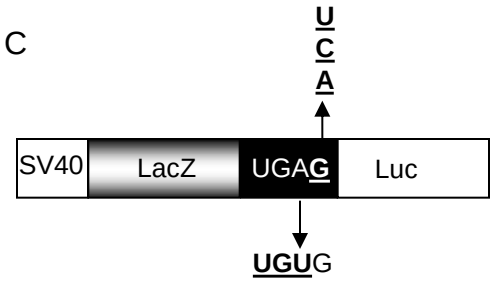
C
UCA
SV40
LacZ
UGAG
Luc
UGUG

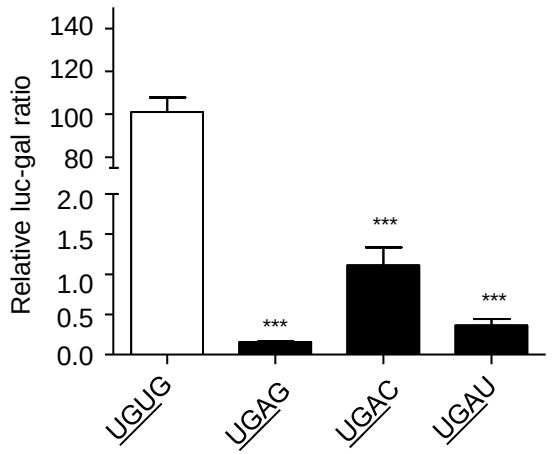
D
Relative luc-gal ratio
140
120
100
80
2.0
1.5
1.0
0.5
0.0
***
***
***
UGUG
UGAG
UGAC
UGAU

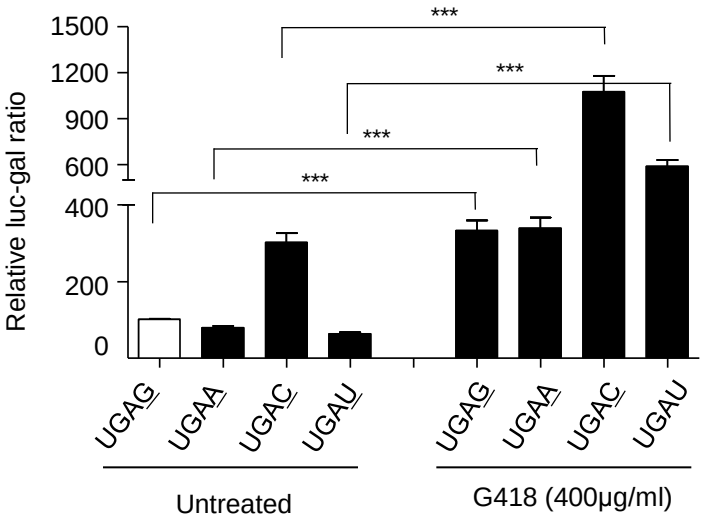
E
Relative luc-gal ratio
1500
1200
900
600
400
200
0
***
***
***
***
UGAG
UGAA
UGAC
UGAU
UGAG
UGAA
UGAC
UGAU
Untreated
G418 (400μg/ml)

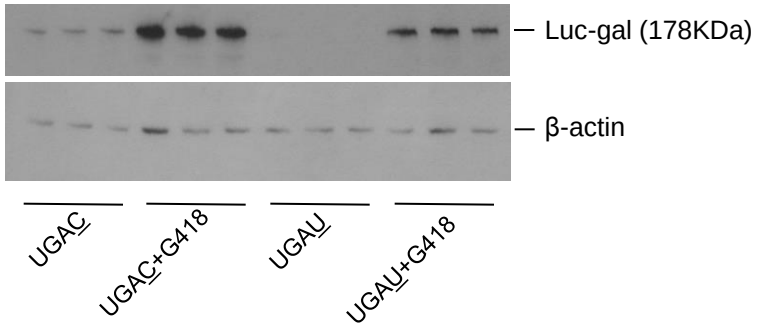
F
Luc-gal (178KDa)
β-actin
UGAC
UGAC+G418
UGAU
UGAU+G418

Figure 2

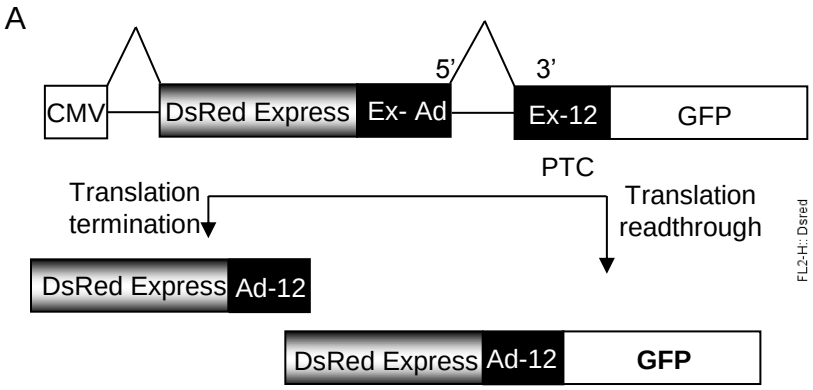
A
CMV
DsRed Express
Ex- Ad
5'
3'
Ex-12
GFP
PTC
Translation termination
Translation readthrough
DsRed Express
Ad-12
DsRed Express
Ad-12
GFP

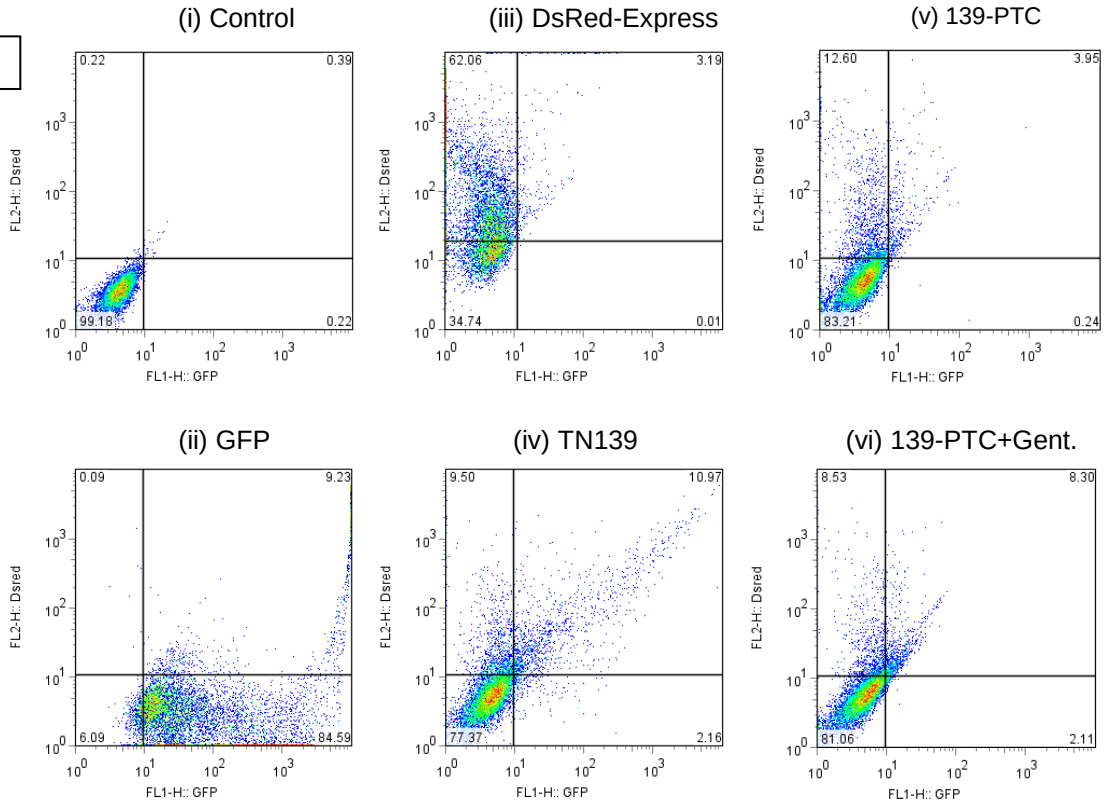
C
(i) Control
(iii) DsRed-Express
(v) 139-PTC
(ii) GFP
(iv) TN139
(vi) 139-PTC+Gent.
FL2-H:: Dsred
FL1-H:: GFP
0.22
0.39
99.18
0.22
62.06
3.19
34.74
0.01
12.60
3.95
83.21
0.24
0.09
9.23
6.09
84.59
9.50
10.97
77.37
2.16
8.53
8.30
81.06
2.11

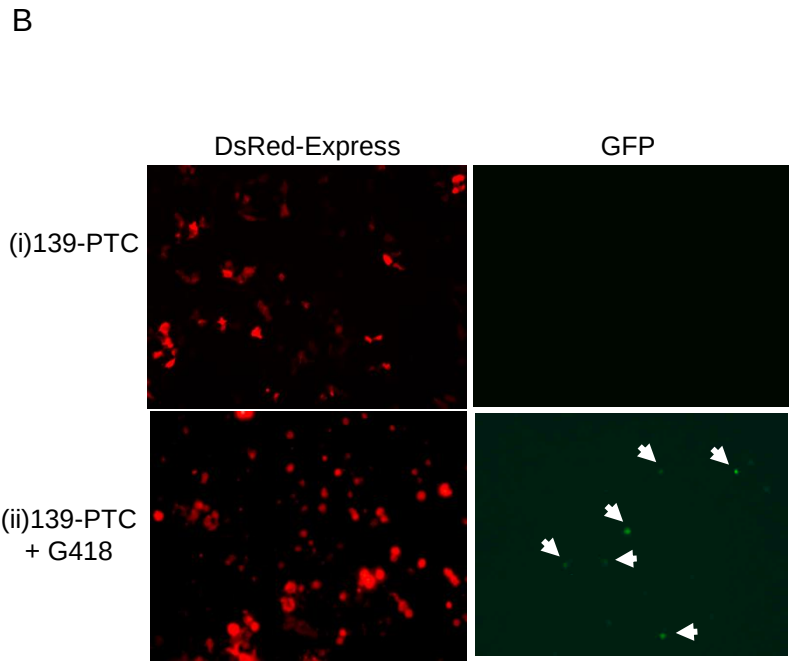
B
DsRed-Express
GFP
(i)139-PTC
(ii)139-PTC
+ G418

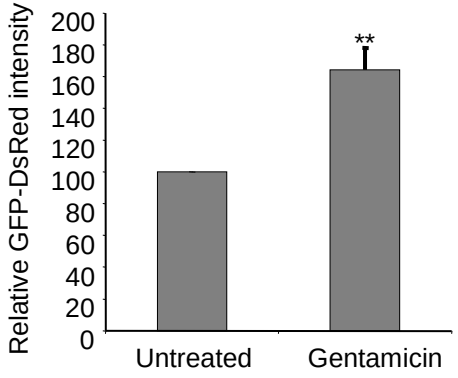
D
Relative GFP-DsRed intensity
200
180
160
140
120
100
80
60
40
20
0
**
Untreated
Gentamicin

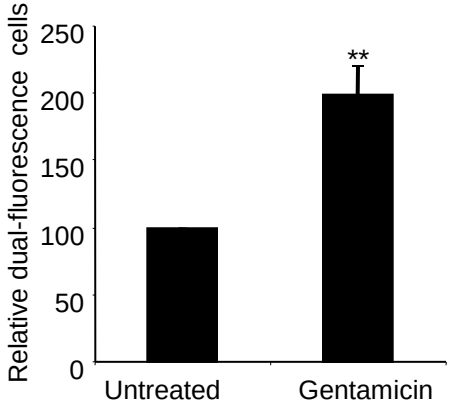
E
Relative dual-fluorescence cells
250
200
150
100
50
0
**
Untreated
Gentamicin

A

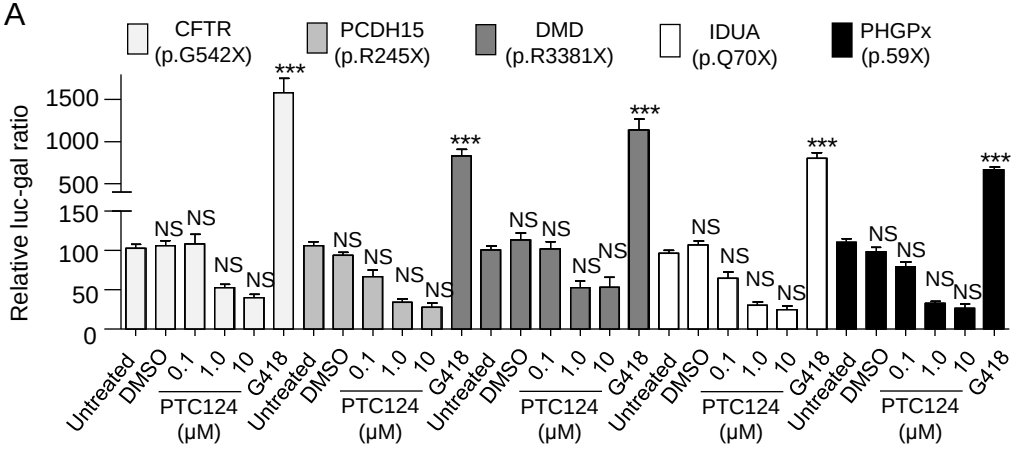
CFTR (p.G542X)
PCDH15 (p.R245X)
DMD (p.R3381X)
IDUA (p.Q70X)
PHGPx (p.59X)
Relative luc-gal ratio
1500
1000
500
150
100
50
0
***
NS
Untreated
DMSO
0.1
1.0
10
G418
PTC124 (μM)

B

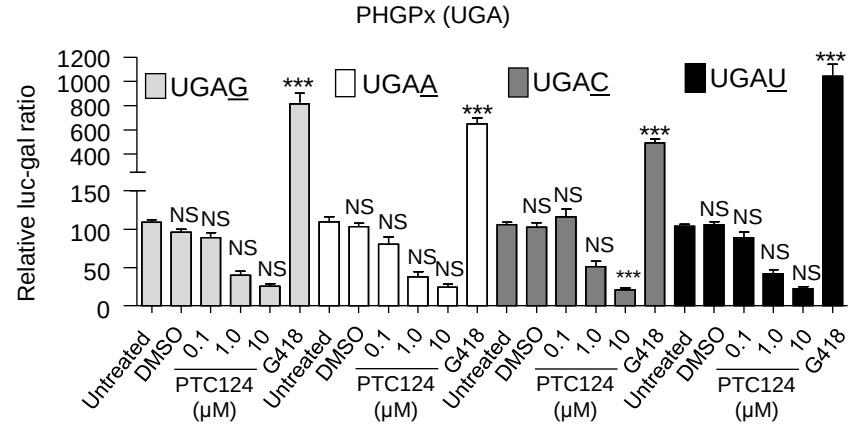
PHGPx (UGA)
UGAG
UGAA
UGAC
UGAU
Relative luc-gal ratio
1200
1000
800
600
400
150
100
50
0
***
NS
Untreated
DMSO
0.1
1.0
10
G418
PTC124 (μM)

C

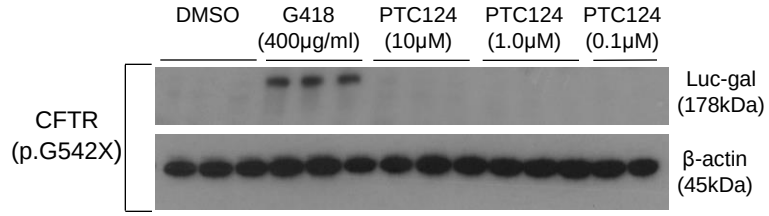
DMSO
G418 (400μg/ml)
PTC124 (10μM)
PTC124 (1.0μM)
PTC124 (0.1μM)
CFTR (p.G542X)
Luc-gal (178kDa)
β-actin (45kDa)

Figure 4

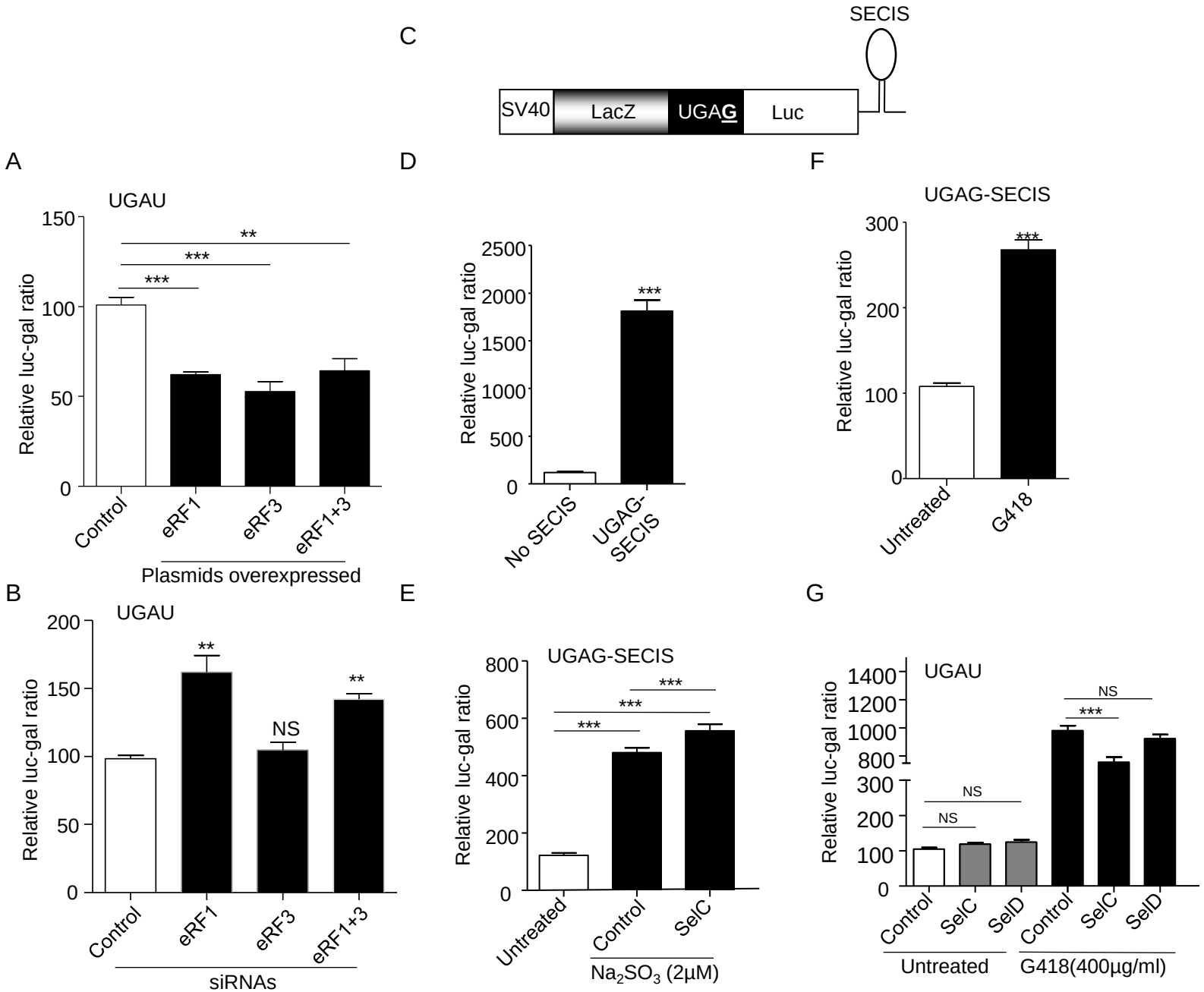
C
SECIS
SV40
LacZ
UGAG
Luc
A
UGAU
Relative luc-gal ratio
150
100
50
0
**
***
***
Control
eRF1
eRF3
eRF1+3
Plasmids overexpressed
D
Relative luc-gal ratio
2500
2000
1500
1000
500
0
***
No SECIS
UGAG-SECIS
F
UGAG-SECIS
Relative luc-gal ratio
300
200
100
0
***
Untreated
G418
B
UGAU
Relative luc-gal ratio
200
150
100
50
0
**
NS
**
Control
eRF1
eRF3
eRF1+3
siRNAs
E
UGAG-SECIS
Relative luc-gal ratio
800
600
400
200
0
***
***
***
Untreated
Control
SelC
Na2SO3 (2μM)
G
UGAU
Relative luc-gal ratio
1400
1200
1000
800
300
200
100
0
NS
NS
NS
***
Control
SelC
SelD
Control
SelC
SelD
Untreated
G418(400μg/ml)

Figure 5

A

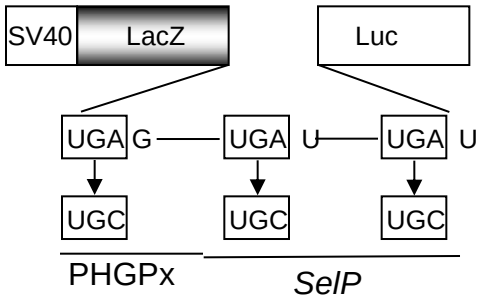

B

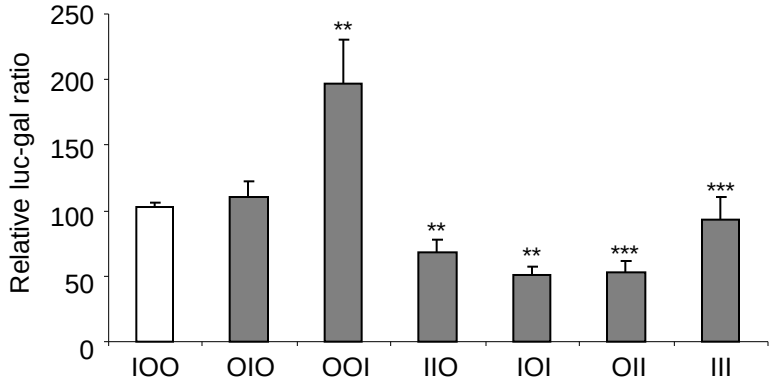

C

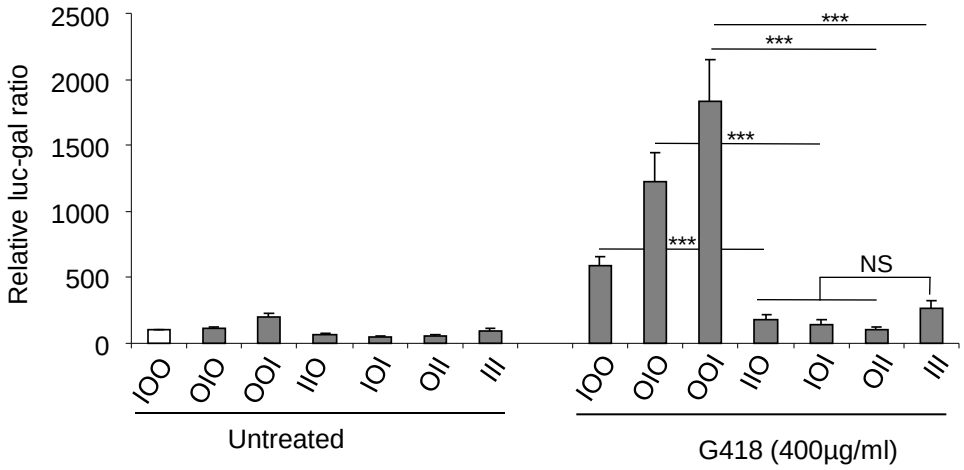

D

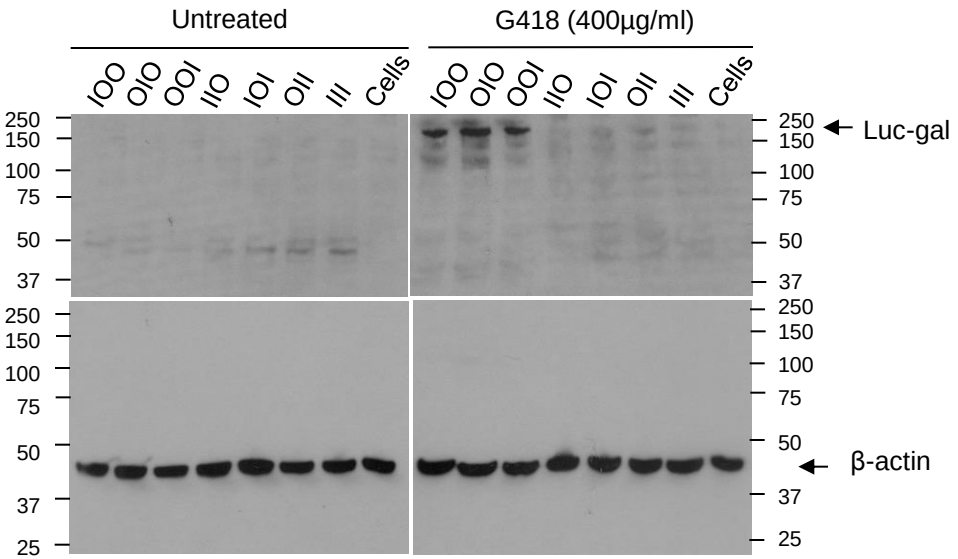

Figure 6

A

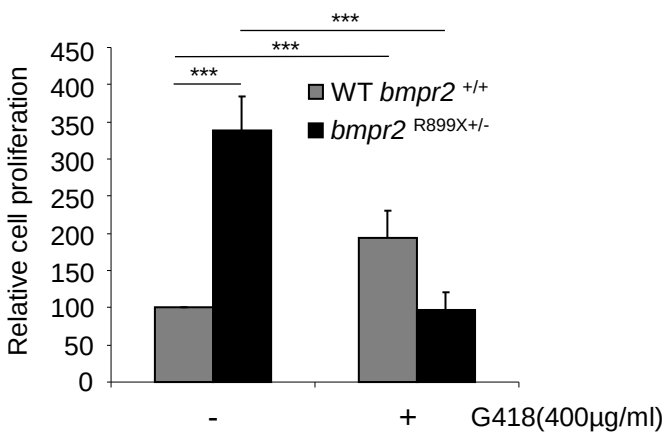
***
***
***
450
400
350
300
250
200
150
100
50
0
Relative cell proliferation
WT bmpr2 +/+
bmpr2 R899X+/-
-
+
G418(400µg/ml)

B

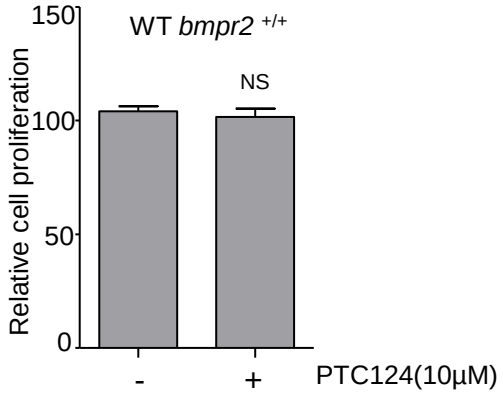
150
100
50
0
Relative cell proliferation
WT bmpr2 +/+
NS
-
+
PTC124(10µM)

C

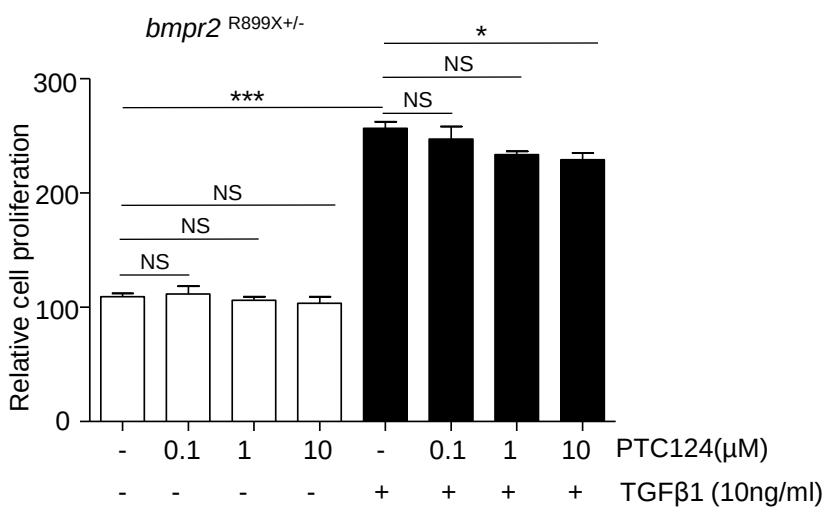
bmpr2 R899X+/-
*
NS
***
NS
NS
NS
NS
300
200
100
0
Relative cell proliferation
- 0.1 1 10 - 0.1 1 10 PTC124(µM)
- - - - + + + + TGFβ1 (10ng/ml)

Figure 7

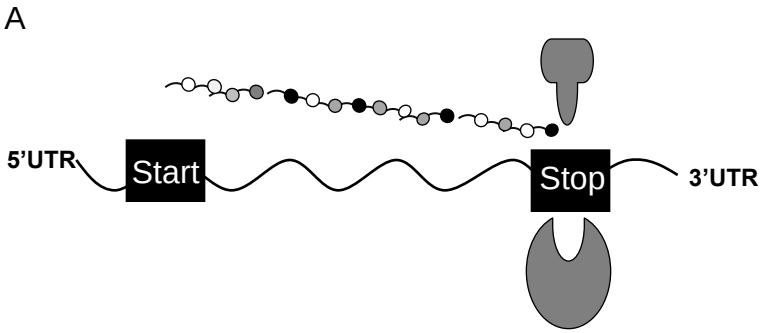
A
5'UTR
Start
Stop
3'UTR

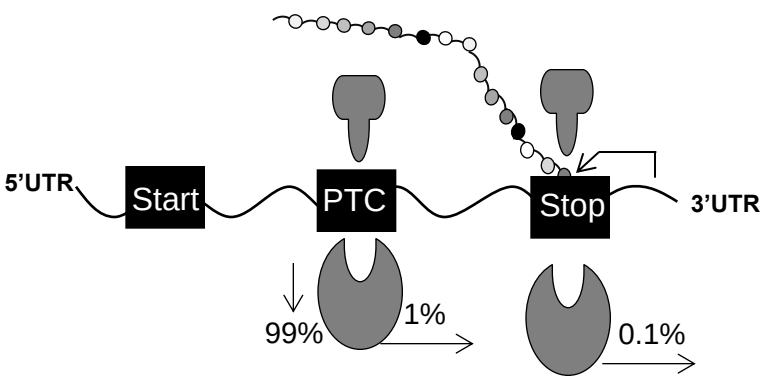
C
5'UTR
Start
PTC
Stop
3'UTR
99%
1%
0.1%

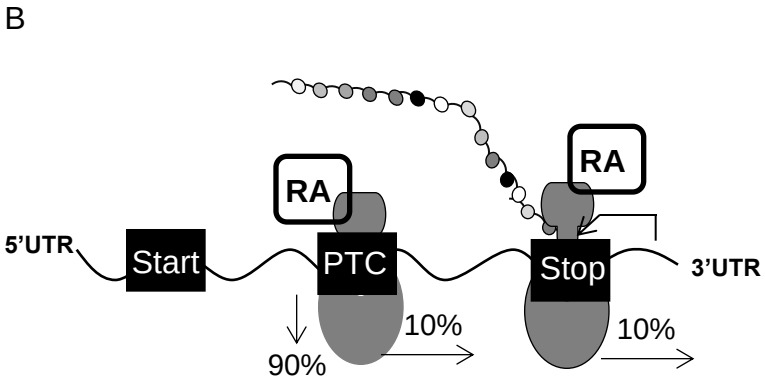
B
RA
RA
5'UTR
Start
PTC
Stop
3'UTR
90%
10%
10%

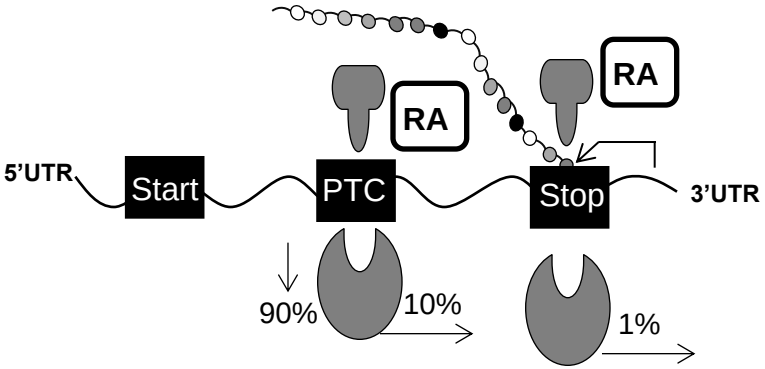
D
RA
RA
5'UTR
Start
PTC
Stop
3'UTR
90%
10%
1%